

Determination of $|V_{cb}|$ using Bayesian analysis of the $B \rightarrow D^* \ell \bar{\nu}_\ell$ semileptonic decay width with four-loop QCD corrections

Wang Li^{1,*}, Xing-Gang Wu^{1,†}, Hua Zhou^{2,‡} and Xu-Chang Zheng^{1,§}

¹*Department of Physics, Chongqing Key Laboratory for Strongly Coupled Physics, Chongqing University, Chongqing 401331, P.R. China*

²*School of Mathematics and Physics, Southwest University of Science and Technology, Mianyang 621010, P.R. China*

The Cabibbo-Kobayashi-Maskawa matrix element $|V_{cb}|$ is an important Standard Model parameter, whose value can be determined by using the semi-leptonic decay $B \rightarrow D^* \ell \bar{\nu}_\ell$. The perturbative QCD (pQCD) corrections to the $B \rightarrow D^*$ transform form factor $\mathcal{F}(w)$ has been known up to the N³LO level, whose magnitude remains sensitive to the choice of renormalization scale μ_r . To improve the precision of $\mathcal{F}(w)$ and hence $|V_{cb}|$, we first apply the single-scale approach of Principle of Maximum Conformality (PMC) to eliminate the conventional (Conv.) renormalization scale dependence of the short-distance parameter η_A and then predict the contribution of its unknown N⁴LO term via Bayesian analysis. In this paper, we adopt two probabilistic models for Bayesian analysis: the Cacciari-Houdeau model (CH model) and the geometric behavior model (GB model). It is shown that by using the PMC series in combination with Bayesian analysis, one can achieve high degree of reliability in estimating unknown higher-order terms. A more convergent behavior is achieved by applying the PMC, confirmed by the predicted N⁴LO contributions: for the CH model, $\eta_A|_{\text{Conv.}}^{\text{N}^4\text{LO}} = \{-0.0032, +0.0052\}$ and $\eta_A|_{\text{PMC}}^{\text{N}^4\text{LO}} = \{-0.0004, +0.0004\}$; for the GB model, $\eta_A|_{\text{Conv.}}^{\text{N}^4\text{LO}} = \{-0.0049, +0.0075\}$ and $\eta_A|_{\text{PMC}}^{\text{N}^4\text{LO}} = \{-0.0007, +0.0007\}$. Comparing with the latest experimental measurements, we obtain $|V_{cb}|_{\text{PMC}} = (40.58^{+0.53}_{-0.57}) \times 10^{-3}$, which is consistent for both CH and GB models and in good agreement with the PDG world average, $|V_{cb}|_{\text{PDG}} = (41.1 \pm 1.2) \times 10^{-3}$ within errors.

I. INTRODUCTION

The Cabibbo-Kobayashi-Maskawa (CKM) matrix elements are essential components of the Standard Model (SM), describing the mixing of quark flavors [1]. Their precise determination is crucial for testing the SM's validity and deepening our understanding of flavor structure. In particular, a precise determination of the CKM matrix element $|V_{cb}|$ is vital for reducing the uncertainties of the unitary triangle and improving predictive accuracy in flavor physics – especially for indirect CP violation, which is highly sensitive to new physics signals. Among these, the semileptonic decay process $B \rightarrow D^* \ell \bar{\nu}_\ell$ ($\ell = e, \mu$) is pivotal for precise extraction of $|V_{cb}|$. In recent years, both the LHC and B factories have provided increasingly precise measurements of the differential decay width and related observables for the $B \rightarrow D^* \ell \bar{\nu}_\ell$ process [2–7]. Theoretically, the differential decay width of the exclusive process $B \rightarrow D^* \ell \bar{\nu}_\ell$ can be expressed as [8]

$$\begin{aligned} \frac{d\Gamma}{dw}(B \rightarrow D^* \ell \bar{\nu}_\ell) &= \frac{G_F^2}{48\pi^3} (m_B - m_{D^*})^2 m_{D^*}^3 \\ &\times \chi(w) (w^2 - 1)^{\frac{1}{2}} |V_{cb}|^2 \\ &\times |\eta_{\text{EW}}|^2 |\mathcal{F}(w)|^2, \end{aligned} \quad (1)$$

where G_F is the Fermi constant, and m_{B,D^*} denotes the mass of the B and D^* meson, respectively. The recoil pa-

rameter w is defined as $w = (m_B^2 + m_{D^*}^2 - q^2)/(2m_B m_{D^*})$. The term $|\eta_{\text{EW}}|$ refers to the electroweak correction factor, and $\mathcal{F}(w)$ represents the transition form factor associated with this process. While $\chi(w)$ denotes an additional phase-space factor, whose expression is [8]:

$$\begin{aligned} \chi(w) &= (w+1)^2 \\ &\times \left(1 + \frac{4w}{w+1} \frac{m_B^2 - 2wm_B m_{D^*} + m_{D^*}^2}{(m_B - m_{D^*})^2} \right) \end{aligned} \quad (2)$$

The parameter $|V_{cb}|$, an important input to Eq.(1), can be extracted by comparing the experimentally measured differential decay width with the theoretically calculated transition form factor $\mathcal{F}(w)$. Therefore, a precise determination of $|\mathcal{F}(w)|$ is crucial for the accurate extraction of $|V_{cb}|$. Using the QCD factorization method, $\mathcal{F}(w)$ can be expressed as $\mathcal{F}(w) = \eta_A \hat{\xi}(w)$, where η_A and $\hat{\xi}(w)$ represent the perturbative short-distance coefficient and long-distance hadronic dynamics [9], respectively. In heavy quark effective theory [10, 11], the long-distance hadronic dynamics $\hat{\xi}(w)$ corresponds to the Isgur-Wise function, normalized such that $\hat{\xi}(1) = 1 + \delta_{1/m_Q^2}$, where Q denotes a heavy quark (b or c).

Currently, the short-distance coefficient η_A has been calculated up to next-to-next-to-next-to-leading order (N³LO) QCD corrections [12]. However, the N³LO series still exhibits significant renormalization scale (μ_r) dependence. Conventionally, μ_r is set to a typical value (e.g., Q) to suppress large logarithmic terms in the expansion coefficients and then varied within a range, e.g., $[Q/n, nQ]$ (where $n = 2, 3, 4, \dots$), to estimate theoretical uncertainties. This scale-setting procedure is inherently arbitrary, leading to a mismatch between the

* lwang@stu.cqu.edu.cn

† wuxg@cqu.edu.cn

‡ zhouhua@swust.edu.cn

§ zhengxc@cqu.edu.cn

perturbative expansion and the strong coupling constant $\alpha_s(\mu_r)$ and causing the pQCD series to depend on the chosen μ_r . Moreover, this renormalization scale uncertainty violates the requirements of renormalization group invariance (RGI) and degrades the accuracy of theoretical predictions.

The Principle of Maximum Conformality (PMC) offers a process-independent method to eliminate conventional renormalization-scale ambiguities and reveal the perturbative nature of the QCD series [13–17]. The scale-running behavior of α_s is governed by the renormalization group equation (RGE). Leveraging this, the PMC approach systematically absorbs all RGE-involved $\{\beta_i\}$ -terms of the series to determine the accurate magnitude of the strong coupling, ensuring a consistent fixed-order pQCD expansion¹. The resulting perturbative coefficients become μ_r -independent and exhibit conformal properties. Notably, the PMC-improved series, with accurate α_s value, is also renormalization-scheme invariant [19–22], which is also ensured by the commensurate scale relations among the pQCD approximants under different schemes [23].

The μ_r -independent PMC series also facilitates the estimation of unknown higher-order (UHO) terms [24–26]. In the 1990s, the Padé approximation approach (PAA) was used to calculate UHO terms [27, 28], where PAA employs the rational generating function to approximate the known finite-term power series and infers UHO terms via series expansion. Ref. [29] utilized a [0,2]-type generating function to estimate the N⁴LO term for η_A , yielding a highly accurate prediction of $|V_{cb}|$. As another innovative attempt, Bayesian analysis (BA) has emerged as an efficient method for estimating UHO contributions [30–32]. BA calculates UHO terms using probability density distributions, specifically by constructing probability distributions and iteratively updating probabilities as new information becomes available. The BA approach has been successfully applied in various high-energy processes [33–35]. In this paper, we use conformal coefficients obtained via the PMC single-scale approach (PMCs) [36, 37] and apply BA to estimate the N⁴LO term of η_A , then incorporate the improved high-precision η_A into the extraction of $|V_{cb}|$.

The rest of the paper is organized as follows. In Sec. II, we sketch the methods used in the calculation, e.g., the PMCs approach and the Bayesian approach. In Sec. III, we present the numerical results and discussions. Sec. IV is reserved as a summary.

II. CALCULATION METHOD

A. The principle of maximum conformality

The perturbative expression of η_A up to N³LO-level QCD corrections can be written as:

$$\eta_A = 1 + \sum_{i=1}^3 r_i a_s^i(\mu_r), \quad (3)$$

where $a_s = \alpha_s/\pi$. This perturbative series is commonly calculated under the $\overline{\text{MS}}$ scheme (the scheme used to define α_s), e.g., Ref. [12]. However, as observed in Ref. [29], the physical V scheme [38–41], which is defined in the static potential between a heavy quark and a heavy antiquark, is more effective than the $\overline{\text{MS}}$ scheme for η_A . In the V scheme, the small scale problem can be avoided and the convergence of this perturbative series can be improved. Thus, in the following calculations, we work in the V scheme. The expansion coefficients r_i under the V scheme can be found in Ref. [29].

By using the QCD degeneracy relations [42], the expansion coefficients r_i can be decomposed into conformal and non-conformal parts:

$$r_1 = r_{1,0}, \quad (4)$$

$$r_2 = r_{2,0} + \beta_0 r_{2,1}, \quad (5)$$

$$r_3 = r_{3,0} + \beta_1 r_{2,1} + 2\beta_0 r_{3,1} + \beta_0^2 r_{3,2}. \quad (6)$$

Based on RGE, the PMCs resums all known types of $\{\beta_i\}$ -terms and determines an overall effective value of α_s (and hence its PMC scale). According to the standard PMCs procedure [36, 37] the pQCD approximant of η_A becomes free of RGE-involved $\{\beta_i\}$ -terms:

$$\eta_{A|\text{PMCs}} = 1 + \sum_{i=1}^3 r_{i,0} a_s^i(Q_*), \quad (7)$$

where $r_{i,0}$ are conformal coefficients and the PMC scale Q_* of the $B \rightarrow D^* \ell \bar{\nu}_\ell$ decay can be determined up to next-to-leading logarithm (NLL) accuracy,

$$\ln \left(\frac{Q_*^2}{Q^2} \right) = T_0 + T_1 a_s(Q), \quad (8)$$

where Q represents the typical momentum flow of the process, which is usually set as $\sqrt{m_b m_c}$ for the present process. The explicit expressions for the expansion coefficients r_i , $r_{i,0}$ and T_i can be found in the Ref. [29].

B. The Bayesian analysis approach

We will estimate the contribution of the unknown N⁴LO term by using the probability distribution, i.e., the BA approach, to derive a more accurate pQCD result. The BA approach serves as an effective approach

¹ If there exist additional $\{\beta_i\}$ -terms associated with other scale-dependent parameters (e.g., parton distribution functions and running quark masses), these terms should be retained as “conformal” ones when determining the magnitude of α_s but will be utilized to fix the appropriate magnitudes of these parameters via their respective RGEs [18].

for constructing probability distributions, founded on the Bayesian theorem and using known information about the perturbative series to create a probability model. When the convergence of the perturbation series is good, the BA approach has high efficiency and predicts reasonable UHO contribution even by using lower fixed-order series. In the paper, we will adopt two Bayesian models, namely the Cacciari-Houdeau (CH) model [30] and the geometric behavior (GB) model [31], to analyze the contribution of the unknown $N^4\text{LO}$ term to η_A and discuss their uncertainties in detail.

1. CH model

The CH model is one of the earliest probabilistic models developed in 2010 for predicting UHO terms, it stands out as one of the most understandable and widely adopted models. A physical quantity that has been calculated up to order a_s^n can be written as:

$$\rho_n = \sum_{i=0}^n c_i a_s^i. \quad (9)$$

There are three hypotheses in the CH model:

- The model assumes that all the coefficients c_i of the perturbative series are bounded in absolute value by a common parameter \bar{c} . The logarithm of \bar{c} is described by a flat probability distribution over the entire parameter space, i.e.,

$$g(\ln \bar{c}) = \frac{1}{2|\ln \epsilon|} \theta(|\ln \epsilon| - |\ln \bar{c}|), \quad (10)$$

where $\theta(x)$ is the Heaviside step function, and the parameter ϵ is taken to the limit $\epsilon \rightarrow 0$ at the end. Here, assigning a flat distribution to $\ln \bar{c}$ reflects the absence of prior knowledge about the order of magnitude of \bar{c} . Then such distribution can be expressed as the probability distribution of \bar{c} :

$$g_0(\bar{c}) = \frac{1}{2|\ln \epsilon|} \frac{1}{\bar{c}} \theta\left(\frac{1}{\epsilon} - \bar{c}\right) \theta(\bar{c} - \epsilon). \quad (11)$$

- With the parameter \bar{c} known, the conditional probability for an unknown coefficient c_k – referred to as the likelihood probability – is given as a uniform distribution in the CH model, i.e.,

$$h_0(c_k|\bar{c}) = \frac{1}{2\bar{c}} \theta(\bar{c} - |c_k|). \quad (12)$$

- The model also assumes that the coefficients are independent from each other, which implies that

$$h(c_i, c_j|\bar{c}) = h_0(c_i|\bar{c})h_0(c_j|\bar{c}). \quad (13)$$

Using the Bayesian conditional probability formula, the probability distribution for an uncalculated coefficient c_k is

$$\begin{aligned} f_c(c_k|c_0, \dots, c_n) &= \frac{f(c_k, c_0, \dots, c_n)}{f(c_0, \dots, c_n)} (k > n) \\ &= \frac{\int d\bar{c} h_0(c_k|\bar{c}) h_0(c_0|\bar{c}) \cdots h_0(c_n|\bar{c}) g_0(\bar{c})}{\int d\bar{c} h_0(c_0|\bar{c}) \cdots h_0(c_n|\bar{c}) g_0(\bar{c})}. \end{aligned} \quad (14)$$

Inserting Eq.(11) and Eq.(12) into Eq.(14), one obtains

$$f_c(c_k|c_0, \dots, c_n) = \begin{cases} \frac{(n+1)}{2(n+2)\bar{c}_{(n)}}, & |c_k| \leq \bar{c}_{(n)} \\ \frac{(n+1)\bar{c}_{(n)}^{(n+1)}}{2(n+2)|c_k|^{n+2}}, & |c_k| > \bar{c}_{(n)} \end{cases} \quad (15)$$

where c_0, \dots, c_n are the known coefficients of the perturbative series, and $\bar{c}_{(n)} = \max(|c_0|, \dots, |c_n|)$. It is observed that Eq.(13) is symmetric about the origin, this indicates that we are generally unable to know the positive or negative nature of the UHO terms.

In Bayesian analysis, one can use the probability distribution equation described above to calculate c_k at a specific degree of confidence, referred to as degree-of-belief (DoB). This interval is known as the credible interval (CI), and its corresponding definition is given by [25]:

$$p\% = \int_{-c_k^{(p)}}^{c_k^{(p)}} f_c(c_k|c_0, \dots, c_n) dc_k, \quad (16)$$

and the distribution interval for the unknown coefficients c_k with a specific DoB can be determined:

$$c_k^{(p)} = \begin{cases} \bar{c}_{(n)} \frac{n+2}{n+1} p\%, & p\% \leq \frac{n+1}{n+2} \\ \bar{c}_{(n)} [(n+2)(1-p\%)]^{-\frac{1}{n+1}}, & p\% > \frac{n+1}{n+2} \end{cases} \quad (17)$$

2. GB model

Another Bayesian model adopted in this paper is the GB model [31]. In the GB model, a standard perturbative series up to order a_s^n is expressed as follows:

$$\rho_n = \rho_0 \sum_{k=0}^n \delta_k, \quad (18)$$

where

$$\delta_k \equiv \frac{\rho_k - \rho_{k-1}}{\rho_0}, \quad (19)$$

denotes the ratio of the difference between the $(k+1)$ -term series and the k -term series to the first term of the series.

The fundamental assumptions of this model are:

- The terms δ_k are bounded by

$$|\delta_k| \leq c a^k, \quad (20)$$

where symbols c and a are hidden parameters of the model that do not appear in the final calculations. Unlike the CH model, the assumption of the GB model does not incorporate the information of the coupling constant α_s , instead, it is included in the δ_k . In the GB model, the corresponding prior probability distribution for c is given by:

$$g_0(c) = \frac{\epsilon}{c^{1+\epsilon}} \theta(c-1), \quad (21)$$

where ϵ is typically a very small positive value. The prior probability distribution of a is given by:

$$g_0(a) = (1+\omega)(1-a)^\omega \theta(a) \theta(1-a), \quad (22)$$

where ω is an integer greater than 1.

- If the probability distribution of c and a are known, the probability distribution for a term δ_k is assumed as:

$$h_0(\delta_k|c, a) = \frac{1}{2c a^k} \theta(c a^k - |\delta_k|). \quad (23)$$

- The terms δ_k are independent from each other, i.e.,

$$h(\delta_i, \delta_j|c, a) = h_0(\delta_i|c, a) h_0(\delta_j|c, a). \quad (24)$$

Using Bayesian theorem, one can obtain the distribution of the first UHO term:

$$f_\delta(\delta_{n+1}|\delta_n, \dots, \delta_1) = \frac{f(\delta_{n+1}, \delta_n, \dots, \delta_1)}{f(\delta_n, \dots, \delta_1)}, \quad (25)$$

where

$$= \int dc \int da h(\delta_m, \dots, \delta_1|c, a) g_0(c) g_0(a). \quad (26)$$

Inserting Eqs.(21-24) into Eq.(25) yields its probability distribution. The calculation based on the GB model can be carried out using the program THunc [31].

Having the probability distribution for UHO terms, the DoB is

$$p\% = \int_{-\delta_{n+1}^{(p)}}^{\delta_{n+1}^{(p)}} f_\delta(\delta_{n+1}|\delta_1, \dots, \delta_n) d\delta_{n+1}. \quad (27)$$

Then, the CI $\delta_{n+1}^{(p)}$ under a specific DoB can be determined using this formula.

III. NUMERICAL RESULTS AND DISCUSSIONS

In this section, we present the numerical results for η_A and $|V_{cb}|$. In the numerical calculation, the pole masses are taken as $m_c = 1.68$ GeV and $m_b = 4.78$ GeV, and the QCD asymptotic scale parameter is taken as $\Lambda_{\text{QCD}|n_f=4}^V = 283.0_{-15.6}^{+16.1}$ MeV² for the V-scheme strong coupling constant [29].

The numerical results for η_A up to N³LO QCD corrections under the conventional (Conv.) and PMCs approaches are

$$\eta_A|_{\text{Conv.}}^{\mu_r=Q/2} = \{1, -0.0953, 0.0921, -0.0259\}, \quad (28)$$

$$\eta_A|_{\text{Conv.}}^{\mu_r=Q} = \{1, -0.0625, -0.0093, -0.0017\}, \quad (29)$$

$$\eta_A|_{\text{Conv.}}^{\mu_r=2Q} = \{1, -0.0475, -0.0336, -0.0319\}, \quad (30)$$

$$\eta_A|_{\text{PMCs.}} = \{1, -0.0644, -0.0158, 0.0027\}. \quad (31)$$

In conventional scale-setting approach, the central value of μ_r is set as $Q = \sqrt{m_b m_c}$. Then, the variation of μ_r within the range $[Q/2, 2Q]$ sets the upper and lower bounds of the theoretical error, leading to significant μ_r uncertainty. It is found that the conventional series does show strong scale dependence, leading to quite different perturbative behaviors. In contrast, the PMC approach systematically removes the conventional renormalization scale uncertainty, and the value of η_A remains invariant under renormalization scale variations. This enables the scale-invariant PMC conformal series to more effectively estimate the contribution of UHO terms.

A. The estimated magnitude of unknown N⁴LO-terms using PAA

In the literature, the PAA has been employed to estimate the contributions of UHO terms. For a comparison, we first present the estimate of unknown N⁴LO-terms based on the PAA. For a perturbative series ρ_n , e.g., given in Eq.(9), the approximation function of PAA can be expressed as follows [27]:

$$\rho_n^{[N/M]} = \frac{p_0 + p_1 a_s + \dots + p_N a_s^N}{1 + q_1 a_s + \dots + q_M a_s^M}, \quad (32)$$

where N and M (with $N + M = n$) denote the highest powers of the numerator and denominator polynomials, respectively, while p_i and q_i are input parameters. By

² The error in $\Lambda_{\text{QCD}|n_f=4}^V$ originates from the uncertainty in the strong coupling constant under the $\overline{\text{MS}}$ scheme, $\alpha_s(M_Z) = 0.1179 \pm 0.0009$ [43]. Specifically, the $\overline{\text{MS}}$ -scheme uncertainty in $\alpha_s(M_Z)$ yields $\Lambda_{\text{QCD}|n_f=4}^{\overline{\text{MS}}} = 207.2_{-11.4}^{+11.8}$ MeV, which in turn propagates to $\Lambda_{\text{QCD}|n_f=4}^V = 283.0_{-15.6}^{+16.1}$ MeV.

comparing the Taylor expansion series of fractional generating function (32) with the original series in Eq.(9) up to order a_s^n , the coefficients p_i and q_i can be uniquely determined via the given series. Subsequently, one can expand Eq.(32) to a higher order, e.g., order a_s^{n+1} , to have an estimation of the uncalculated a_s^{n+1} term.

	$\eta_A _{\text{Conv.}}^{\text{N}^4\text{LO}}$	$\eta_A _{\text{PMCs}}^{\text{N}^4\text{LO}}$
[0/3]-type	$0.0044^{+0.0106}_{+0.0040}$	0.0001
[1/2]-type	$-0.0301^{+0.0123}_{-0.0290}$	0.0001
[2/1]-type	$-0.0003^{+0.0075}_{-0.0299}$	-0.0005

TABLE I. The predictions for the N^4LO term of η_A , estimated using the three types of PAA under both the conventional and PMCs approaches, show that the error in the conventional series arises from the renormalization scale with $\mu_r \in [Q/2, 2Q]$.

Up to now, the perturbative series of η_A is known up to N^3LO -level; there are three types of PAA, namely [0/3], [1/2], and [2/1]. Uncertainties of different $[N/M]$ -types can be treated as the systematic errors of the PAA method itself. The predicted N^4LO coefficient c_4 by the three types are as follows:

$$c_4^{[0/3]} = \frac{c_1^4 - 3c_0 c_1^2 c_2 + c_0^2 c_2^2 + 2c_0^2 c_1 c_3}{c_0^3}, \quad (33)$$

$$c_4^{[1/2]} = \frac{-c_2^3 + 2c_1 c_2 c_3 - c_0 c_3^2}{c_1^2 - c_0 c_2}, \quad (34)$$

$$c_4^{[2/1]} = \frac{c_3^2}{c_2}. \quad (35)$$

The estimated values for the N^4LO term of η_A are presented in Table I. The conventional results indicate that different types of PAA result in significant variations of $\eta_A|_{\text{Conv.}}^{\text{N}^4\text{LO}}$. In Table I, the error of the conventional results is caused by taking $\mu_r \in [Q/2, 2Q]$, whose magnitude is $(^{+241\%}_{+91\%})$ for [0/3]-type, $(^{ -41\%}_{+96\%})$ for [1/2]-type, and $(^{+250\%}_{-9967\%})$ for [2/1]-type, respectively. For the subsequent discussion, we will use the squared average of the results of the three types as the final prediction. Compared to the conventional scale-setting approach, the PMCs not only substantially reduces the μ_r uncertainty but also achieves consistent predictions across three distinct types of PAA. This significantly enhances the predictive accuracy of the N^4LO term.

B. The estimated magnitude of unknown N^4LO -terms using CH model of BA

We now present the numerical results based on the two BA models in terms of a probability distribution. Applying the CH model to η_A with the 95% DoB, we obtain the estimate for the CI of higher order coefficients. The estimated coefficients are presented in Table II. The

results for c_i are estimated based on the known coefficients $(c_0, c_1, \dots, c_{i-1})$. These intervals for coefficients are symmetric about the zero.

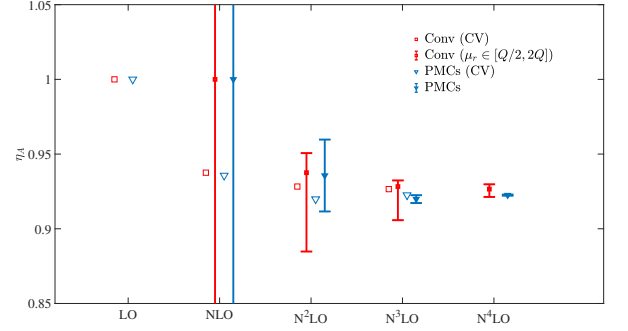


FIG. 1. Comparison of the calculated central values of η_A for the known series (labeled as “CV”) with the predicted CIs (with DoB=95%) of η_A up to N^4LO level. The red hollow squares and blue hollow triangles represent the calculated central values of the known fixed-order pQCD predictions under conventional and PMCs approaches, respectively. The red square, blue triangle, and their corresponding error bars represent the BA (CH model) predictions for η_A under conventional and PMC approaches, respectively.

In Fig.1, we present a comparison between the central values of η_A calculated using the known series and the CIs (with DoB=95%) of η_A predicted based on the CH model. The predicted η_A at the NLO level falls within the range of an interval but carries significant uncertainty, this is due to the fact that we have less known information about the coefficients when $n = 0$. With the increase of order, the CI of η_A is greatly reduced. For example, compared to the estimated CI at the N^3LO level, the estimated CI of η_A at the N^4LO level is reduced by a factor of four. Furthermore, the scale dependence ($\mu_r \in [Q/2, 2Q]$) of the conventional approach leads to a widening of the coefficient prediction interval, resulting in a large uncertainty for η_A . On the contrary, the uncertainties of the PMCs results are much smaller, e.g., the CI of η_A at the N^4LO level almost converges to one point. Therefore, the PMCs approach greatly improves the accuracy of the prediction to the N^4LO term. In Table III, we also provide detailed numerical results for the N^4LO term of η_A for further illustration.

We also present the probability density distribution of η_A after using the PMCs approach and the CH model in Fig.2. The four lines in Fig.2 correspond to different levels: given LO (solid line), given NLO (dashed line), given N^2LO (dotted line), and given N^3LO (dotted-dashed line). The prominent shapes of those curves indicate the highest possibility of the η_A values. Their shapes resemble a towering flat straight line at the center, with suppressed tail curves trailing on each side, resulting in an overall symmetric graph. Fig.2 shows that as the known information is updated, the probability of the straight-line portion becomes larger while its interval width decreases, tending to converge to one point. Si-

	c_1	c_2	c_3	c_4
Conv.	$[-10.0000, +10.0000]$	$[-2.5820, +2.5820]$	$[-1.8064, +1.8064]$	$[-2.9504, +2.9504]$
PMCs	$[-10.0000, +10.0000]$	$[-2.5820, +2.5820]$	$[-2.8989, +2.8989]$	$[-4.2332, +4.2332]$

TABLE II. The CI (DoB = 95%) for the coefficients c_i (μ_r) ($i = 1, 2, 3, 4$) at the scale $\mu_r = Q$ under the conventional approach and the scale-invariant coefficients c_i under PMCs approach.

The predicted N^4 LO term of η_A under the CH model	
Conv.	$[-0.0032, +0.0052]$
PMCs	$[-0.0004, +0.0004]$

TABLE III. The predicted N^4 LO term of η_A using the CH model under the PMCs approach and conventional approach, where the initial renormalization scale is taken as the range $\mu_r \in [Q/2, 2Q]$.

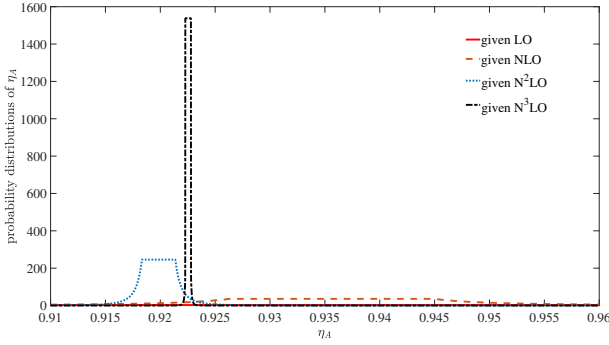


FIG. 2. The probability density distributions of η_A with the PMCs approach under the CH model. The solid line, dashed line, dotted line, dotted-dashed line are results for the given LO, NLO, N^2 LO, and N^3 LO series, respectively.

multaneously, the probability of the curved portions on each side gradually converges to zero.

C. The estimated magnitude of unknown N^4 LO-terms using GB model of BA

By using the GB model with the parameters $\epsilon = 0.01$ and $\omega = 2$ to the perturbative series of η_A , we obtain its UHO contributions, which are depicted in Fig.3. The figure shows that the results from the conventional scale-setting approach bring large renormalization scale uncertainty. In contrast, the results from the PMCs approach do not have this uncertainty. It can be observed that, as the amount of known perturbative information increases, the CIs (DoB = 95%) significantly decrease. Additionally, the results from the N^4 LO term indicate that the prediction intervals nearly overlap at certain point, aligning well with the characteristics of the GB model. It is notable that the results from each order are encapsulated within the results from the preceding order, demonstrat-

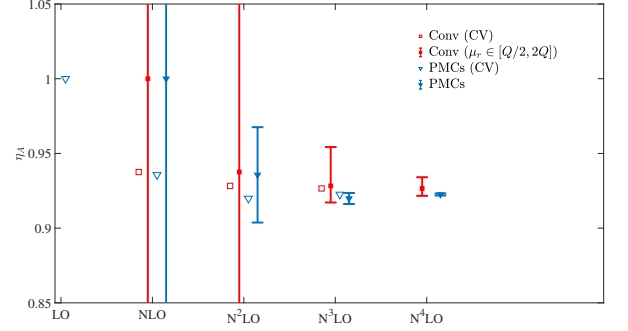


FIG. 3. Under the GB model, the predicted CI with the typical 95% DoB for the η_A by the conventional scale-setting approach (where the renormalization scale $\mu_r \in [Q/2, 2Q]$) and PMCs approach, respectively.

ing the strong convergence of the GB model.

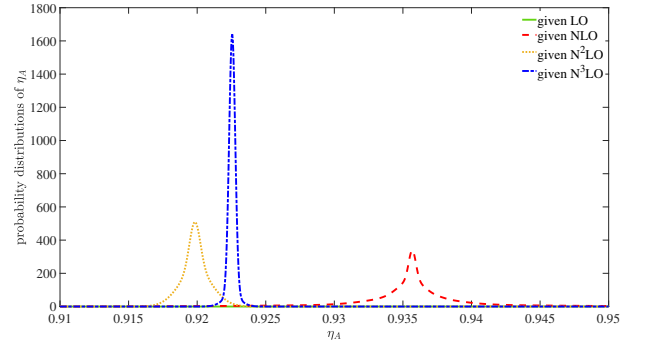


FIG. 4. The probability density distributions of η_A with different orders of knowledge predicted by PMCs under the GB model. The solid line, long dashed line, dotted line and dashed-dotted line are results for the given LO, NLO, N^2 LO and N^3 LO series, respectively.

To better understand the above results, we also present the probability distribution of η_A under the GB model in Fig.4. For the case of only LO being known, the distribution manifests as a straight line nearly overlapping the x -axis, leading to an infinite standard deviation – indicating that predictions based on known first-order information alone yield invalid results. When NLO, N^2 LO, and N^3 LO are considered, the functions are all symmetric curves with a central bump, resulting in the mean and median coinciding. As the number of known orders increases, η_A becomes increasingly concentrated around the distribution's center, leading to smaller standard devia-

The predicted N ⁴ LO term of η_A under the GB model	
Conv.	$[-0.0049, +0.0075]$
PMCs	$[-0.0007, +0.0007]$

TABLE IV. The predicted N⁴LO term of η_A using the GB model under the conventional scale-setting (within the scale range $\mu_r \in [Q/2, 2Q]$) and the PMCs approaches.

tions and narrower prediction intervals for higher-order terms. Compared to the distributions in Fig. 2, the GB model's probability distribution function shares many similarities with that of the CH model. The key distinction is that the GB model's central peak is a single point rather than a flat distribution, signifying a value with the highest probability – where the UHO contribution is zero. Detailed numerical results for the N⁴LO term of η_A are presented in Table IV.

	$\eta_A(\text{Conv.})$	$\eta_A(\text{PMCs})$
[0/3]-type	$0.9265^{+0.0458}_{-0.0408}$	$0.9225^{+0.0112}_{-0.0162}$
[1/2]-type	$0.9265^{+0.0460}_{-0.0508}$	$0.9225^{+0.0112}_{-0.0162}$
[2/1]-type	$0.9265^{+0.0450}_{-0.0508}$	$0.9225^{+0.0112}_{-0.0162}$

TABLE V. The values of η_A using three types of PAA under the conventional and PMCs approaches.

	$\eta_A(\text{Conv.})$	$\eta_A(\text{PMCs})$
CH model	$0.9265^{+0.0446}_{-0.0412}$	$0.9225^{+0.0113}_{-0.0162}$
GB model	$0.9265^{+0.0451}_{-0.0411}$	$0.9225^{+0.0113}_{-0.0162}$

TABLE VI. The values of η_A using the CH and GB Bayesian models under the conventional and PMCs approaches.

In addition to the uncertainty caused by UHO terms, there is also uncertainty caused by the value of $\alpha_s(M_Z)$ in the $\overline{\text{MS}}$ scheme. Using $\alpha_s(M_Z) = 0.1179 \pm 0.0009$ [43], we obtain $\Lambda_{\text{QCD}|n_f=4}^V = 283.0^{+16.1}_{-15.6}$ MeV [29]. Combining the uncertainties from the renormalization scale, the UHO terms and $\alpha_s(M_Z)$, we obtain the final values of η_A . The numerical results of η_A are presented in Table V and Table VI. Notably, the numerical results for PMCs appear to be almost the same across both tables. This consistency is due to the fact that the contributions from higher orders of PMCs series are minimal, thereby exerting an almost negligible effect on η_A .

To facilitate the final numerical analysis, we take the average of the data in Table V and Table VI for discussion. Subsequently, we obtain the following results:

$$\eta_A|_{\text{Conv.}}^{\text{PAA}} = 0.9265^{+0.0456}_{-0.0477}, \quad (36)$$

$$\eta_A|_{\text{PMCs}}^{\text{PAA}} = 0.9225^{+0.0113}_{-0.0162}, \quad (37)$$

$$\eta_A|_{\text{Conv.}}^{\text{Bayes}} = 0.9265^{+0.0448}_{-0.0412}, \quad (38)$$

$$\eta_A|_{\text{PMCs}}^{\text{Bayes}} = 0.9225^{+0.0113}_{-0.0162}. \quad (39)$$

Then, using the heavy quark effective theory, $|\mathcal{F}(1)| = \hat{\xi}(1)\eta_A$, where $\hat{\xi}(1)$ have been calculated in Refs. [44–46], and δ_{1/m_Q^2} is about $-(5.5 \pm 2.5)\%$, the value of $|\mathcal{F}(1)|$ can be obtained. To extract the value of $|V_{cb}|$, we adopt the Caprini, Lellouch, and Neubert (CLN) parameterization [47] for the form factor $\mathcal{F}(w)$, and use the experimental data from various experimental groups [48–54]. The extracted values of $|V_{cb}|$ are presented in Table VII.

It demonstrates that the results from PMCs approach exhibit smaller theoretical uncertainties and higher precision compared to those from the conventional scale-setting approach. The $|V_{cb}|_{\text{PMCs}}^{\text{PAA}}$ are basically the same as $|V_{cb}|_{\text{PMCs}}^{\text{Bayes}}$. However, by comparing $|V_{cb}|_{\text{Conv.}}^{\text{PAA}}$ and $|V_{cb}|_{\text{Conv.}}^{\text{Bayes}}$, it is evident that the results from the Bayesian models have smaller uncertainties. The weighted average of these theoretical values can be calculated by the formula in Ref. [55]:

$$\bar{x} \pm \delta\bar{x} = \frac{\sum_i w_i x_i}{\sum_i w_i} \pm \left(\sum_i w_i \right)^{-1/2}, \quad (40)$$

where \bar{x} represents the central value, $\delta\bar{x}$ stands for its uncertainty, and $w_i = 1/(\delta_i x_i)^2$ is the weight factor. Then we obtain the weighted average of $|V_{cb}|$:

$$|V_{cb}|_{\text{Conv.}}^{\text{PAA}} = (40.83^{+0.90}_{-0.92}) \times 10^{-3}, \quad (41)$$

$$|V_{cb}|_{\text{PMCs}}^{\text{PAA}} = (40.58^{+0.53}_{-0.57}) \times 10^{-3}, \quad (42)$$

$$|V_{cb}|_{\text{Conv.}}^{\text{Bayes}} = (40.82^{+0.89}_{-0.84}) \times 10^{-3}, \quad (43)$$

$$|V_{cb}|_{\text{PMCs}}^{\text{Bayes}} = (40.58^{+0.53}_{-0.57}) \times 10^{-3}. \quad (44)$$

The above results agree with the PDG average value, i.e., $|V_{cb}|_{\text{PDG}} = (41.1 \pm 1.2) \times 10^{-3}$ [56], within errors. As a comparison, the recent value reported by HFLAV is $|V_{cb}|_{\text{HFLAV}} = (38.90 \pm 0.53) \times 10^{-3}$ [57]. This value deviates from the PDG average value by 0.89σ , and deviates from the four predicted values by 0.85σ , 1.13σ , 1.00σ , and 1.13σ , respectively.

IV. SUMMARY

In this paper, we provide an analysis of the parameter η_A for the process $B \rightarrow D^* \ell \bar{\nu}_\ell$ up to the N⁴LO level. The N⁴LO term of η_A was estimated using Bayesian models (the CH and GB models) based on the available pQCD series up to N³LO. For comparison, the N⁴LO term was also estimated using the conventional PAA approach. We found that the uncertainties in predictions from the Bayesian models are reduced compared to those from the PAA under the conventional scale-setting approach. However, due to the enhanced convergence of the η_A series after applying the PMCs, the predictions of the N⁴LO term were largely consistent between the PAA and Bayesian models under the PMCs approach. The results show that the PMCs approach effectively enhances the precision of theoretical predictions

	$ V_{cb} _{\text{PMCs}}^{\text{PAA}}$	$ V_{cb} _{\text{Conv.}}^{\text{PAA}}$	$ V_{cb} _{\text{PMCs}}^{\text{Bayes}}$	$ V_{cb} _{\text{Conv.}}^{\text{Bayes}}$
OPAL partial reco [48]	$42.72^{+1.85}_{-1.93}$	$42.83^{+2.76}_{-2.83}$	$42.72^{+1.85}_{-1.93}$	$42.83^{+2.73}_{-2.60}$
OPAL excl [48]	$40.84^{+2.37}_{-2.43}$	$40.94^{+3.08}_{-3.14}$	$40.84^{+2.37}_{-2.43}$	$40.94^{+3.05}_{-2.95}$
DELPHI partial reco [49]	$40.67^{+1.21}_{-1.31}$	$40.77^{+2.29}_{-2.37}$	$40.67^{+1.21}_{-1.31}$	$40.77^{+2.26}_{-2.12}$
DELPHI excl [50]	$39.94^{+1.19}_{-1.29}$	$40.04^{+2.25}_{-2.33}$	$39.94^{+1.19}_{-1.29}$	$40.04^{+2.22}_{-2.08}$
BABAR excl [51]	$39.53^{+1.20}_{-1.30}$	$39.63^{+2.24}_{-2.32}$	$39.53^{+1.20}_{-1.30}$	$39.63^{+2.21}_{-2.08}$
BABAR D^{*0} [52]	$40.90^{+1.37}_{-1.47}$	$41.00^{+2.39}_{-2.47}$	$40.90^{+1.37}_{-1.47}$	$41.00^{+2.36}_{-2.23}$
BABAR global fit [53]	$40.44^{+1.98}_{-2.05}$	$40.54^{+2.77}_{-2.84}$	$40.44^{+1.98}_{-2.05}$	$40.54^{+2.75}_{-2.64}$
BELLE [54]	$41.92^{+2.19}_{-2.26}$	$42.03^{+2.97}_{-3.04}$	$41.92^{+2.19}_{-2.26}$	$42.03^{+2.95}_{-2.84}$

TABLE VII. The values of $|V_{cb}|(\times 10^{-3})$ using $\eta_A|_{\text{Conv.}}^{\text{PAA}}$, $\eta_A|_{\text{PMCs}}^{\text{PAA}}$, $\eta_A|_{\text{Conv.}}^{\text{Bayes}}$, and $\eta_A|_{\text{PMCs}}^{\text{Bayes}}$, which are derived from the data given by various experiment groups [48–54] and under CLN parameterization [47].

by eliminating scale uncertainty relative to the conventional approach. Finally, by comparing the theoretical prediction of the decay width for $B \rightarrow D^* \ell \bar{\nu}_\ell$ with the latest experimental measurements, we obtained $|V_{cb}|_{\text{PMC}} = (40.58^{+0.53}_{-0.57}) \times 10^{-3}$, which is in good agreement with the PDG world average value $|V_{cb}|_{\text{PDG}} = (41.1 \pm 1.2) \times 10^{-3}$.

Acknowledgments: This work was supported by the Natural Science Foundation of China under Grants No.12175025 and No.12347101, by the Research Fund for the Doctoral Program of the Southwest University of Science and Technology under Contract No.24zx7117 and No.23zx7122, and by the Chongqing Natural Science Foundation under Grant No. CSTB2022NSCQ-MSX0415.

-
- [1] T. Matsuoka, The CKM matrix and its origin, Prog. Theor. Phys. **100**, 107-122 (1998).
- [2] D. Buskulic *et al.* [ALEPH], A measurement of $|V_{cb}|$ from $B^0 \rightarrow D^{*+} \ell^- \nu_\ell$, Phys. Lett. B **359**, 236-248 (1995).
- [3] K. Abe *et al.* [Belle], Measurement of $B(\bar{B}^0 \rightarrow D^+ \ell^- \bar{\nu})$ and determination of $|V_{cb}|$, Phys. Lett. B **526**, 258-268 (2002).
- [4] D. Buskulic *et al.* [ALEPH], Measurements of $|V_{cb}|$, form factors and branching fractions in the decays $B^0 \rightarrow D^{*+} \ell^- \nu_\ell$ and $B^0 \rightarrow D^+ \ell^- \nu_\ell$, Phys. Lett. B **395**, 373-387 (1997).
- [5] K. Abe *et al.* [Belle], Determination of $|V_{cb}|$ using the semileptonic decay $B^0 \rightarrow D^{*+} e^- \nu$, Phys. Lett. B **526**, 247-257 (2002).
- [6] S. Jaiswal, S. Nandi and S. K. Patra, Extraction of $|V_{cb}|$ from $B \rightarrow D^{(*)} \ell \nu_\ell$ and the Standard Model predictions of $R(D^{(*)})$, JHEP **12**, 060 (2017).
- [7] K. Ackersstaff *et al.* [OPAL], A measurement of $|V_{cb}|$ using $B^0 \rightarrow D^{*+} \ell^- \nu_\ell$ decays, Phys. Lett. B **395**, 128-140 (1997).
- [8] G. Ricciardi and M. Rotondo, Determination of the Cabibbo-Kobayashi-Maskawa matrix element $|V_{cb}|$, J. Phys. G **47**, 113001 (2020).
- [9] M. Neubert, Theoretical update on the model independent determination of $|V_{cb}|$ using heavy quark symmetry, Phys. Lett. B **338**, 84-91 (1994).
- [10] A. V. Manohar and M. B. Wise, Heavy quark physics, Camb. Monogr. Part. Phys. Nucl. Phys. Cosmol. **10**, 1-191 (2000).
- [11] M. E. Luke, Effects of subleading operators in the heavy quark effective theory, Phys. Lett. B **252**, 447-455 (1990).
- [12] J. P. Archambault and A. Czarnecki, Three-loop QCD corrections and b-quark decays, Phys. Rev. D **70**, 074016 (2004).
- [13] S. J. Brodsky and X. G. Wu, Scale Setting Using the Extended Renormalization Group and the Principle of Maximum Conformality: the QCD Coupling Constant at Four Loops, Phys. Rev. D **85**, 034038 (2012).
- [14] S. J. Brodsky and L. Di Giustino, Setting the Renormalization Scale in QCD: The Principle of Maximum Conformality, Phys. Rev. D **86**, 085026 (2012).
- [15] S. J. Brodsky and X. G. Wu, Eliminating the Renormalization Scale Ambiguity for Top-Pair Production Using the Principle of Maximum Conformality, Phys. Rev. Lett. **109**, 042002 (2012).
- [16] M. Mojaza, S. J. Brodsky and X. G. Wu, Systematic All-Orders Method to Eliminate Renormalization-Scale and Scheme Ambiguities in Perturbative QCD, Phys. Rev. Lett. **110**, 192001 (2013).
- [17] S. J. Brodsky, M. Mojaza and X. G. Wu, Systematic Scale-Setting to All Orders: The Principle of Maximum Conformality and Commensurate Scale Relations, Phys. Rev. D **89**, 014027 (2014).
- [18] J. Yan, X. G. Wu, J. M. Shen, X. D. Huang and Z. F. Wu, Scale-invariant total decay width $\Gamma(H \rightarrow b\bar{b})$ using the novel method of characteristic operator, JHEP **04**, 184 (2025).
- [19] X. G. Wu, Y. Ma, S. Q. Wang, H. B. Fu, H. H. Ma, S. J. Brodsky and M. Mojaza, Renormalization Group Invariance and Optimal QCD Renormalization Scale-Setting, Rept. Prog. Phys. **78**, 126201 (2015).
- [20] X. G. Wu, S. Q. Wang and S. J. Brodsky, Importance of proper renormalization scale-setting for QCD testing at

- colliders, *Front. Phys. (Beijing)* **11**, 111201 (2016).
- [21] X. G. Wu, J. M. Shen, B. L. Du, X. D. Huang, S. Q. Wang and S. J. Brodsky, The QCD renormalization group equation and the elimination of fixed-order scheme-and-scale ambiguities using the principle of maximum conformality, *Prog. Part. Nucl. Phys.* **108**, 103706 (2019).
 - [22] J. Yan, S. J. Brodsky, L. Di Giustino, P. G. Ratcliffe, S. Wang, S. Q. Wang, X. Wu and X. G. Wu, The Principle of Maximum Conformality Correctly Resolves the Renormalization-Scheme-Dependence Problem, *Symmetry* **17**, 411 (2025).
 - [23] S. J. Brodsky and H. J. Lu, Commensurate scale relations in quantum chromodynamics, *Phys. Rev. D* **51**, 3652 (1995).
 - [24] B. L. Du, X. G. Wu, J. M. Shen and S. J. Brodsky, Extending the Predictive Power of Perturbative QCD, *Eur. Phys. J. C* **79**, 182 (2019).
 - [25] J. M. Shen, Z. J. Zhou, S. Q. Wang, J. Yan, Z. F. Wu, X. G. Wu and S. J. Brodsky, Extending the predictive power of perturbative QCD using the principle of maximum conformality and the Bayesian analysis, *Eur. Phys. J. C* **83**, 326 (2023).
 - [26] Z. F. Wu, X. G. Wu, J. Yan, X. D. Huang and J. M. Shen, A new method for estimating unknown one-order higher QCD corrections to the perturbative series using the linear regression through the origin, [arXiv:2505.05131 [hep-ph]].
 - [27] M. A. Samuel, J. R. Ellis and M. Karliner, Comparison of the Pade approximation method to perturbative QCD calculations, *Phys. Rev. Lett.* **74**, 4380-4383 (1995).
 - [28] M. A. Samuel, G. Li and E. Steinfelds, Estimating perturbative coefficients in quantum field theory using Pade approximants.2, *Phys. Lett. B* **323**, 188 (1994).
 - [29] H. Zhou, Q. Yu, X. C. Zheng, H. B. Fu and X. G. Wu, New determination of $|V_{cb}|$ using the three-loop QCD corrections for the $B \rightarrow D^*$ semi-leptonic decays, *Nucl. Phys. A* **1030**, 122595 (2023).
 - [30] M. Cacciari and N. Houdeau, Meaningful characterisation of perturbative theoretical uncertainties, *JHEP* **09**, 039 (2011).
 - [31] M. Bonvini, Probabilistic definition of the perturbative theoretical uncertainty from missing higher orders, *Eur. Phys. J. C* **80**, 989 (2020).
 - [32] C. Duhr, A. Huss, A. Mazeliauskas and R. Szafron, An analysis of Bayesian estimates for missing higher orders in perturbative calculations, *JHEP* **09**, 122 (2021).
 - [33] Y. F. Luo, J. Yan, Z. F. Wu and X. G. Wu, Approximate N⁵LO Higgs Boson Decay Width $\Gamma(H \rightarrow \gamma\gamma)$, *Symmetry* **16**, 173 (2024).
 - [34] J. M. Shen, B. H. Qin, J. Yan, S. Q. Wang and X. G. Wu, Novel method to reliably determine the QCD coupling from R_{uds} measurements and its effects to $\mu\alpha - 2$ and $\alpha(M_Z^2)$ within the tau-charm energy region, *JHEP* **07**, 109 (2023).
 - [35] J. Yan, X. G. Wu, H. Zhou, H. T. Li and J. H. Shan, Improved analysis of the decay width of $t \rightarrow Wb$ up to N³LO QCD corrections, *Phys. Rev. D* **109**, 114026 (2024).
 - [36] J. M. Shen, X. G. Wu, B. L. Du and S. J. Brodsky, Novel All-Orders Single-Scale Approach to QCD Renormalization Scale-Setting, *Phys. Rev. D* **95**, 094006 (2017).
 - [37] J. Yan, Z. F. Wu, J. M. Shen and X. G. Wu, Precise perturbative predictions from fixed-order calculations, *J. Phys. G* **50**, 045001 (2023).
 - [38] T. Appelquist, M. Dine and I. J. Muzinich, The Static Potential in Quantum Chromodynamics, *Phys. Lett. B* **69**, 231-236 (1977).
 - [39] W. Fischler, Quark - anti-Quark Potential in QCD, *Nucl. Phys. B* **129**, 157-174 (1977).
 - [40] M. Peter, The Static quark - anti-quark potential in QCD to three loops, *Phys. Rev. Lett.* **78**, 602-605 (1997).
 - [41] Y. Schroder, The Static potential in QCD to two loops, *Phys. Lett. B* **447**, 321-326 (1999).
 - [42] H. Y. Bi, X. G. Wu, Y. Ma, H. H. Ma, S. J. Brodsky and M. Mojaza, Degeneracy Relations in QCD and the Equivalence of Two Systematic All-Orders Methods for Setting the Renormalization Scale, *Phys. Lett. B* **748**, 13-18 (2015).
 - [43] R. L. Workman *et al.* [Particle Data Group], Review of Particle Physics, *PTEP* **2022**, 083C01 (2022).
 - [44] M. Neubert, Uncertainties in the determination of $-V(cb)$, [arXiv:hep-ph/9505238 [hep-ph]].
 - [45] P. Gambino, T. Mannel and N. Uraltsev, $B \rightarrow D^*$ at zero recoil revisited, *Phys. Rev. D* **81**, 113002 (2010).
 - [46] P. Gambino, T. Mannel and N. Uraltsev, $B \rightarrow D^*$ zero-recoil formfactor and the heavy quark expansion in QCD: a systematic study, *JHEP* **10**, 169 (2012).
 - [47] I. Caprini, L. Lellouch and M. Neubert, Dispersive bounds on the shape of anti- $B \rightarrow D^{(*)}$ lepton anti-neutrino form-factors, *Nucl. Phys. B* **530**, 153-181 (1998).
 - [48] G. Abbiendi *et al.* [OPAL], Measurement of $|V_{cb}|$ using $\bar{B}^0 \rightarrow D^{*+} \ell^- \nu$ decays, *Phys. Lett. B* **482**, 15-30 (2000).
 - [49] P. Abreu *et al.* [DELPHI], Measurement of V_{cb} from the decay process $\bar{B}^0 \rightarrow D^{*+} \ell^- \bar{\nu}$, *Phys. Lett. B* **510**, 55-74 (2001).
 - [50] J. Abdallah *et al.* [DELPHI], Measurement of $|V_{cb}|$ using the semileptonic decay $\bar{B}_d^0 \rightarrow D^{*+} \ell^- \bar{\nu}_\ell$, *Eur. Phys. J. C* **33**, 213-232 (2004).
 - [51] B. Aubert *et al.* [BaBar], Determination of the form-factors for the decay $B^0 \rightarrow D^{*-} \ell^+ \nu_\ell$ and of the CKM matrix element $|V_{cb}|$, *Phys. Rev. D* **77**, 032002 (2008).
 - [52] B. Aubert *et al.* [BaBar], Measurement of the Decay $B^- \rightarrow D^{*0} e^- \bar{\nu}_e$, *Phys. Rev. Lett.* **100**, 231803 (2008).
 - [53] B. Aubert *et al.* [BaBar], Measurements of the semileptonic decays $\bar{B} \rightarrow D \ell \bar{\nu}$ and $\bar{B} \rightarrow D^* \ell \bar{\nu}$ using a global fit to $DX \ell \bar{\nu}$ final states, *Phys. Rev. D* **79**, 012002 (2009).
 - [54] E. Waheed *et al.* [Belle], Measurement of the CKM matrix element $|V_{cb}|$ from $B^0 \rightarrow D^{*-} \ell^+ \nu_\ell$ at Belle, *Phys. Rev. D* **100**, 052007 (2019).
 - [55] P. A. Zyla *et al.* [Particle Data Group], Review of Particle Physics, *PTEP* **2020**, 083C01 (2020).
 - [56] S. Navas *et al.* [Particle Data Group], Review of particle physics, *Phys. Rev. D* **110**, 030001 (2024).
 - [57] Y. S. Amhis *et al.* [HFLAV], Averages of b-hadron, c-hadron, and τ -lepton properties as of 2021, *Phys. Rev. D* **107**, 052008 (2023).